The Primordial Lithium Problem

Brian D. Fields

Departments of Astronomy and of Physics, University of Illinois, Urbana, Illinois 61801; email: bdfields@illinois.edu

Annu. Rev. Nucl. Part. Sci. 2011. 61:47–68

First published online as a Review in Advance on May 10, 2011

The *Annual Review of Nuclear and Particle Science* is online at nucl.annualreviews.org

This article's doi: 10.1146/annurev-nucl-102010-130445

0163-8998/11/1123-00047$20.00

Keywords

big bang nucleosynthesis, early universe, dark matter, abundances of light elements, extensions of the Standard Model

Abstract

Big bang nucleosynthesis (BBN) theory, together with the precise WMAP cosmic baryon density, makes tight predictions for the abundances of the lightest elements. Deuterium and ^{4}He measurements agree well with expectations, but ^{7}Li observations lie below the BBN+WMAP prediction by a factor of three to four. This 4–5-σ mismatch constitutes the so-called cosmic lithium problem; disparate solutions are possible. First, astrophysical systematics in the observations could exist but are increasingly constrained. Second, nuclear physics experiments provide a wealth of well-measured cross-section data, but ^{7}Be destruction could be enhanced by unknown or poorly measured resonances. Third, physics beyond the Standard Model could alter the ^{7}Li abundance, although deuterium and ^{4}He must remain unperturbed. In this review, we discuss such scenarios, highlighting decaying supersymmetric particles and time-varying fundamental constants. Present and planned experiments could reveal which (if any) of these proposed solutions is correct.

Contents

1. INTRODUCTION 48
2. STANDARD BIG BANG NUCLEOSYNTHESIS IN LIGHT OF WMAP: THE LITHIUM PROBLEM EMERGES 49
   2.1. Standard Big Bang Nucleosynthesis Theory 49
   2.2. Light-Element Observations 51
   2.3. Microwave Background Anisotropies as a Cosmic Baryometer 54
   2.4. Assessing Standard Big Bang Nucleosynthesis: the Lithium Problem(s) Revealed 55
3. SOLUTIONS TO THE LITHIUM PROBLEM(S) 56
   3.1. Astrophysical Solutions 56
   3.2. Nuclear Physics Solutions 58
   3.3. Solutions Beyond the Standard Model 59
4. DISCUSSION AND OUTLOOK 65

1. INTRODUCTION

Big bang nucleosynthesis (BBN) describes the production of the lightest nuclides—deuterium, ^{3}He, ^{4}He, and ^{7}Li—at times ranging from ~1 s to ~3 min after the big bang. Theoretical predictions of the light-element abundances are well understood and rest on the secure microphysics of nuclear cross sections and Standard Model weak and electromagnetic interactions (1, 2). These predictions are in broad quantitative agreement with measured primordial light-element abundances derived from observations of the local and high-redshift universe. This concordance represents a great success of the hot big bang cosmology and makes BBN our earliest reliable probe of the universe.

BBN has dramatically changed over the past decade in response to the cosmological revolution sparked by a flood of new observations. Notably, WMAP measurements of the cosmic microwave background (CMB) radiation have precisely determined the cosmological baryon and total matter contents (3, 4), and high-redshift supernova observations have revealed that the universe recently entered a phase of accelerated expansion (5–8). These and other observations both reveal the existence and tightly determine the abundance of both dark matter and dark energy on cosmic scales, where they dominate the mass-energy budget of the universe. Yet the nature of both dark matter and dark energy remains unknown. Thus, twenty-first-century cosmology finds itself in a peculiar state of "precision ignorance." This situation is particularly exciting for particle physics because both dark matter and dark energy demand physics beyond the Standard Model.

BBN has played a central role in the development of this new cosmology. CMB data now measure the cosmic baryon density, independently of BBN and with high precision. The CMB results cast BBN in a new light: A comparison between these two measurements of cosmic baryons provides a strong new test of the basic hot big bang framework (9). Moreover, this test can now be performed in a new way, namely through the use of the CMB baryon density as an input to the BBN calculation, which outputs predictions for each light-element abundance. Each of these predictions can then be directly compared with light-element observations (10). The result is that deuterium shows spectacular agreement between BBN+CMB predictions and high-redshift observations, and ^{4}He shows good agreement. However, on the basis of the first-year WMAP

data, ^{7}Li shows a discrepancy of a factor of two to three, which represents a 2–3-σ disagreement between observations and theory (11–14). This disagreement has worsened over time; it now stands at a factor of three to four in abundance, or 4–5 σ. This disagreement is known as the lithium problem.

In this review, we present an overview of the lithium problem that is accessible to nuclear and particle physicists and to astrophysicists. Excellent, broader reviews of primordial nucleosynthesis and its relation to cosmology and particle physics are available elsewhere (2, 15–17).

In Section 2, we trace the origin of the lithium problem, focusing on the physics of BBN ^{7}Li production, the nature and precision of light-element abundance measurements, and the state of light-element concordance in view of the CMB-measured cosmic baryon density. We review possible solutions to the lithium problem in Section 3: (*a*) astrophysical systematic uncertainties in lithium abundances and/or their interpretation; or (*b*) new or revised nuclear physics inputs to the BBN calculation, in the form of increased mass-7 destruction via novel reaction pathways or by resonant enhancement of otherwise minor channels; or (*c*) new physics—either particle processes beyond the Standard Model occurring during or soon after BBN, or large changes to the cosmological framework used to interpret light-element (and other) data. We close by summarizing the near-future outlook in Section 4.

2. STANDARD BIG BANG NUCLEOSYNTHESIS IN LIGHT OF WMAP: THE LITHIUM PROBLEM EMERGES

2.1. Standard Big Bang Nucleosynthesis Theory

The cosmic production of light nuclides is the result of weak and nuclear reactions in the context of an expanding, cooling universe. So-called standard BBN refers to the scenario for light-element production, which marries the Standard Model of particle physics with the ΛCDM (standard cold dark matter) cosmology, which provides for

1. gravity governed by general relativity,
2. a homogeneous and isotropic universe (cosmological principle),
3. the microphysics of the Standard Model of particle physics, and
4. the particle content of the Standard Model, supplemented by dark matter and dark energy.

Under these assumptions, the expansion of the universe is governed by the Freidmann equation

$$\left(\frac{\dot{a}}{a}\right)^2 \equiv H^2 = \frac{8\pi}{3} G\rho, \qquad 1.$$

where $a(t)$ is the dimensionless cosmic scale factor (related to redshift z via $1 + z = 1/a$), and $H = \dot{a}/a$ is the universal expansion rate. The total cosmic mass-energy density $\rho = \sum \rho_i$ sums contributions from all cosmic species i.

By far the largest contribution to the density comes from radiation: relativistic species for which $m \ll T$ (where T is temperature), namely blackbody photons and $N_\nu = 3$ species of neutrinos and antineutrinos, and $e^\pm$ pairs at $T \gtrsim m_e$. Cosmic matter consists of nonrelativistic species with $m \gg T$: nucleons n and p, and e^- when $T \lesssim m_e$. Because $\rho_{\rm rad} \gg \rho_{\rm matter}$, Equation 1 shows that radiation dominates cosmic dynamics during BBN.

BBN occurs entirely in this radiation-dominated epoch, for which the energy density has $\rho \propto T^4$, and $T \propto 1/a$ (adiabatic cooling). This, together with Equation 1, gives $t \propto 1/T^2$, or

$$t \approx 1\,{\rm s}\left(\frac{1\,{\rm MeV}}{T}\right)^2. \qquad 2.$$

Light-element formation depends crucially on the relative amounts of baryons (nucleons) and radiation, which are parameterized by the baryon-to-photon ratio

$$\eta \equiv \frac{n_{\rm b}}{n_\gamma} = 2.74 \times 10^{-8} \Omega_b h^2. \quad 3.$$

Here $\Omega_b = \rho_b/\rho_{\rm crit}$ and $\rho_{\rm crit} = 3H_0^2/8\pi G$, where H_0 is the present expansion rate (Hubble parameter). In standard BBN, η is the only free parameter that controls primordial light-element abundances.

Initially, cosmic baryons take the form of free nucleons, n and p. For $T \gtrsim 1$ MeV, and thus $t \lesssim 1$ s, weak interactions are rapid (rates per nucleon $\Gamma_{n\leftrightarrow p} \gg H$), so

$$n + \nu_e \leftrightarrow p + e^- \quad 4.$$

and

$$p + \bar{\nu}_e \leftrightarrow n + e^+ \quad 5.$$

drive the neutrons and protons to an equilibrium ratio,

$$\frac{n}{p} = e^{-(m_n - m_p)/T}. \quad 6.$$

If we consider the nucleon a two-level system, Equation 6 is simply the Boltzmann ratio of the excited- to ground-state populations.

At $T = T_{\rm f} \approx 1$ MeV, the $n - p$ interconversion (Equations 4 and 5) stops as the weak interaction "freezes out" ($\Gamma_{n\leftrightarrow p} \ll H$), which fixes $n/p \approx e^{-(m_n - m_p)/T_{\rm f}} \sim 1/6$. Deuterium production, $p(n, \gamma)d$, occurs but is stymied by the large number of photons per baryon, $n_\gamma/n_{\rm b} = 1/\eta \sim 10^9$, which leads to effective deuteron photodissociation by the $E_\gamma > B_d = 2.22$ MeV tail of the Planck distribution. During this time, free-neutron decay reduces the neutron-to-proton ratio to $\approx$1/7.

At $T \approx 0.07$ MeV, blackbody photons become ineffective at photodissociating deuterium. The deuteron abundance rapidly rises, and launches a series of reactions in which all of the light elements are built via strong (i.e., nuclear) interactions. The simplified reaction network shown in **Figure 1** highlights the reactions that dominate production of the light nuclides. In contrast to much of stellar nucleosynthesis, for BBN the number of key reactions is small and well defined, and all of the important reactions have been measured in the laboratory at the relevant energies; no low-energy extrapolations are needed.

Figure 2 shows the standard BBN light-element abundances as a function of the single free parameter $\eta_{10} = 10^{10}\eta$ (Equation 3). The ^{4}He abundance is weakly sensitive to η (note that the zero is suppressed in the top-panel abscissa). In contrast, deuterium drops strongly with η, and ^{3}He decreases substantially. The ^{7}Li abundance is plotted after ^{7}Be decay and thus sums both mass-7 species. ^{7}Li production dominates the mass-7 abundance in the low-η regime of the plot, whereas ^{7}Be production dominates at the high-η regime, which leads to the "dip" behavior.

The envelopes around the curves in **Figure 2** correspond to the 1-σ uncertainties in the abundance predictions. These uncertainties are propagated from the error budgets—statistical and systematic—of the 12 dominant reactions shown in **Figure 1** (12, 18–26). The uncertainties in ^{4}He are tiny (<1%), and those in deuterium and ^{3}He are small (~7%), whereas the ^{7}Li uncertainties are larger (~12% in the high-η regime of interest).

Several aspects of lithium production are noteworthy. Mass-7 is produced both as ^{7}Li and as ^{7}Be; the $^7\mathrm{Be} \xrightarrow{\rm EC} {}^7\mathrm{Li}$ electron capture occurs long after BBN ceases (27). The $^3\mathrm{He}(\alpha, \gamma)^7\mathrm{Be}$ channel dominates ^{7}Be production. Destruction occurs via $^7\mathrm{Be}(n, p)^7\mathrm{Li}$, followed by the rapid $^7\mathrm{Li}(p, \alpha)^4\mathrm{He}$ reaction. Finally, ^{6}Li production in standard BBN is very small: $^6\mathrm{Li/H} \simeq 10^{-14}$, or $^6\mathrm{Li}/^7\mathrm{Li} \lesssim 10^{-4}$ (28, 29).

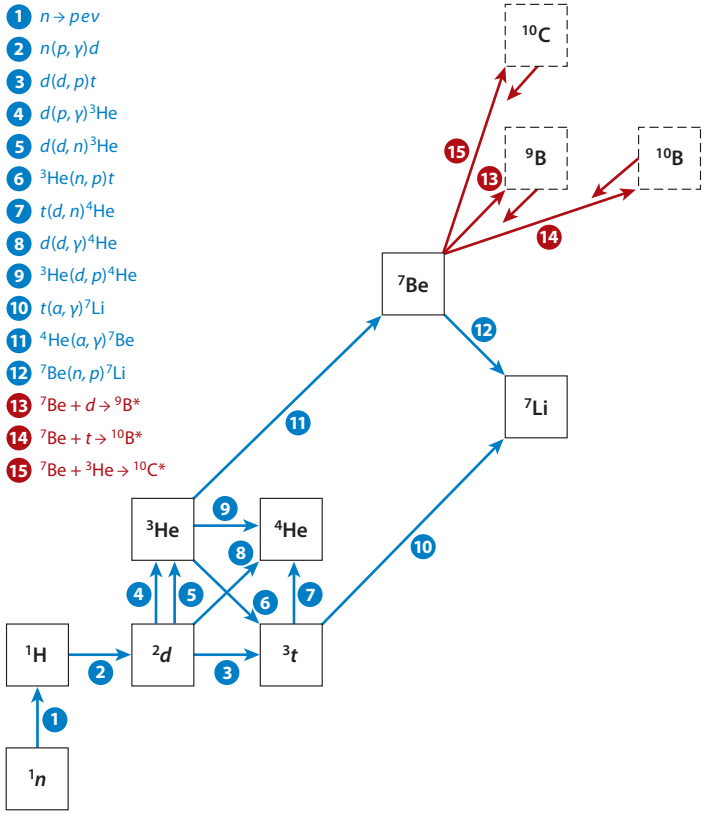

Figure 1

Simplified big bang nucleosynthesis nuclear network. Shown are 12 normally important reactions (*blue*) and 3 proposed or tested new reactions (*red*).

2.2. Light-Element Observations

Measuring the primordial abundance of any light element remains challenging. The BBN levels set at $z \sim 10^{10}$ are reliably accessible only in sites at $z \leq 3$ and often $z \sim 0$. Other nucleosynthesis processes have intervened, as evidenced by the nonzero metallicity of all known astrophysical systems. Thus, one seeks to measure light elements in the most metal-poor systems, then to obtain primordial abundances requires extrapolation to zero metallicity. The below discussion closely follows that of References 30–32.

2.2.1. Deuterium, ^{3}He, and ^{4}He. Deuterium can be measured directly at high redshift. It is present in distant neutral hydrogen gas clouds, which are observed in absorption along sight lines to distant quasars. At present, there are seven systems with robust deuterium measurements (33–38). These lie around redshift $z \sim 3$ and have a metallicity that is $\sim 10^{-2}$ that of solar system material; thus, deuterium should be essentially primordial. For these systems,

$$\frac{\mathrm{D}}{\mathrm{H}} = (2.82 \pm 0.21) \times 10^{-5}, \qquad 7.$$

where the error has been inflated by the reduced $\chi^2_\nu = 2.95$.

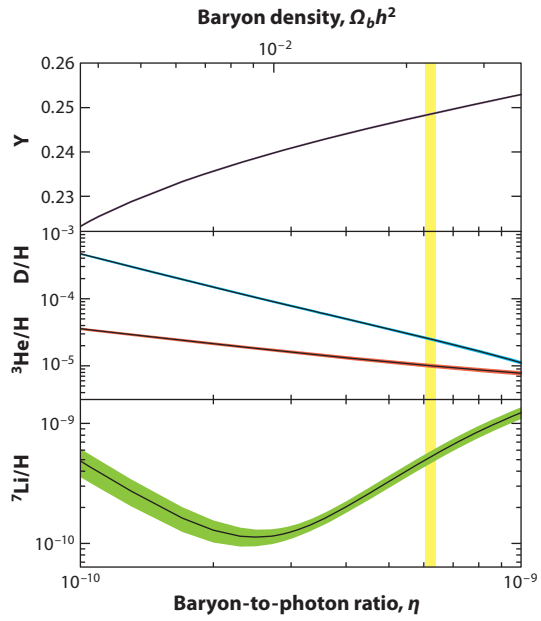

Figure 2

Big bang nucleosynthesis theory predictions for light-element abundances versus the baryon-to-photon ratio η. Curve widths: 1-σ theoretical uncertainties. The vertical yellow band represents the WMAP determination of η. Reproduced from Reference 30.

^{4}He can be measured in emission from nearby metal-poor galaxies (extragalactic HII regions). The challenge is to reliably infer abundances at the needed $\lesssim$1% level. Several recent analyses differ due to systematics in the extraction of abundances from nebular lines (39–43). The mass fraction (40) of

$$Y_p = 0.249 \pm 0.009 \qquad 8.$$

has the largest and most conservative measure of the error budget; the allowed range overlaps with analyses of other groups.

^{3}He is at present accessible only in our Galaxy's interstellar medium (44). This unfortunately means it cannot be measured at low metallicity, and so its primordial abundance cannot be determined reliably (45); we do not use ^{3}He to constrain BBN.

2.2.2. ^{7}Li. Lithium is measured in the atmospheres of metal-poor stars in the stellar halo (Population II) of our Galaxy. Due to convective motions, surface material can be dragged to the hot stellar interior, where lithium is burned readily; this effect is evidenced by low lithium abundances in cool halo stars. Fortunately, the hottest (most massive) halo stars have thin convection zones and show no correlation between lithium and temperature. We consider only lithium abundances in these stars.

Figure 3 shows lithium and iron abundances for a sample of halo stars (46). The ratio of lithium to hydrogen (Li/H) is nearly independent of the ratio of iron to hydrogen (Fe/H); this flat trend is known as the Spite plateau in honor of its discoverers (47). However, heavy elements such as iron (metals) increase with time as Galactic nucleosynthesis proceeds and matter cycles in and out of stars. Thus, the Spite plateau indicates that most halo star lithium is uncorrelated with Galactic nulceosynthesis and hence that lithium is primordial.

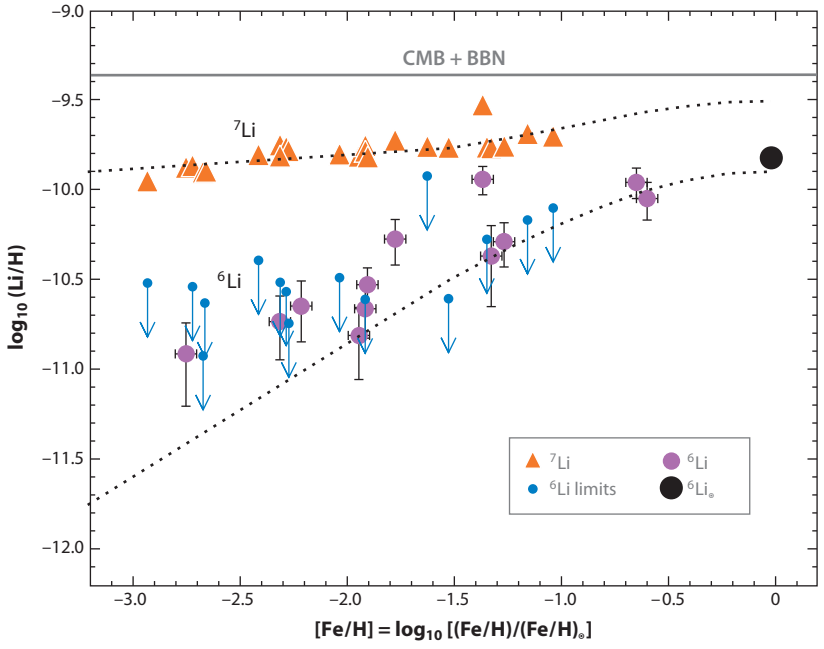

Figure 3

Lithium abundances in selected metal-poor Galactic halo stars. For each star, both lithium isotopes are plotted versus the star's metallicity: [Fe/H] = $\log_{10}[(\mathrm{Fe/H})_{\mathrm{obs}}/(\mathrm{Fe/H})_{\odot}]$. Upper points show ^{7}Li. The flatness of ^{7}Li versus iron is known as the Spite plateau; it indicates that the bulk of the lithium is unrelated to Galactic nucleosynthesis processes and thus is primordial. The horizontal band gives the CMB+WMAP prediction; the gap between this prediction and the plateau illustrates the ^{7}Li problem. Points below the Spite plateau show ^{6}Li abundances; the apparent flatness of these points constitutes the ^{6}Li problem. Curves show predictions of a Galactic cosmic-ray nucleosynthesis model. Points have been corrected for pre-main-sequence depletion. Abbreviation: CMB, cosmic microwave background. Reproduced from Reference 46 with permission.

Moreover, the Spite plateau level measures the primordial abundance. Thanks to the sustained effort of several groups (46, 48–56), a large sample of halo stars have measured lithium abundances. The dominant errors are systematic. A careful attempt to account for the full lithium error budget found (57)

$$\frac{\mathrm{Li}}{\mathrm{H}} = (1.23^{+0.68}_{-0.32}) \times 10^{-10}, \qquad 9.$$

where the 95%-CL error budget is dominated by systematics (see also Section 3.1).

Finally, lithium has now been observed in stars in an accreted metal-poor dwarf galaxy. The Li/H abundances are consistent with the Spite plateau, indicating the plateau's universality (58).

2.2.3. ^{6}Li. Due to the isotope shift in atomic lines, ^{6}Li and ^{7}Li are in principle distinguishable spectroscopically. In practice, the isotopic splitting is several times smaller than the thermal broadening of stellar lithium lines. Nevertheless, the isotopic abundance remains encoded in the detailed shape of the lithium absorption profile.

High–spectral resolution lithium measurements in halo stars attain the precision needed to observe isotope signatures. Some researchers have claimed to detect ^{6}Li with isotopic ratios in the

following range (46):

$$\frac{^6\mathrm{Li}}{^7\mathrm{Li}} \simeq 0.05. \qquad 10.$$

Figure 3 shows the inferred ^{6}Li/H abundance for some of these stars; its independence of metallicity is strikingly reminiscent of the ordinary Spite plateau and, similarly, seems to suggest a primordial origin.

^{6}Li observations remain controversial. It has been argued that stellar convective motions can alter the delicate line shapes and mimic ^{6}Li (59). Thus, there are only a few halo stars for which there is widespread agreement that ^{6}Li has even been detected. The conservative approach is to take the ^{6}Li observations as upper limits, although it will be of interest to learn what is required to explain the ^{6}Li plateau, if it exists. Regardless, the isotopic searches confirm that most of primordial lithium is indeed ^{7}Li, in accord with standard BBN predictions.

2.3. Microwave Background Anisotropies as a Cosmic Baryometer

It is difficult to overstate the cosmological impact of the stunningly precise CMB measurements by WMAP and other experiments. The temperature and polarization anisotropies encode a wealth of cosmological information. Temperature fluctuations robustly record acoustic oscillations of the (re)combining baryon-photon plasma within dark matter potential; for a review, see Reference 60. One of the most precise and robust results is the measurement of the cosmic baryon density and thus of η.

Figure 4 shows the sensitivity of temperature anisotropy to baryon density as a function of angular scale (multipole) on the sky. Generally, increasing baryon density amplifies the odd peaks and depresses the even peaks. Accurate measurements of these peaks by WMAP and other

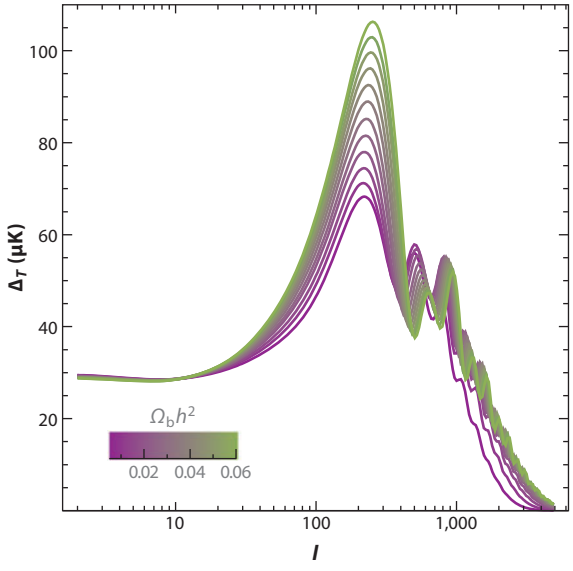

Figure 4

Cosmic microwave background sensitivity to cosmic baryon content. Predictions for temperature anisotropy (root mean square of temperature fluctuation $\Delta_T^2 = \langle T_\ell \rangle^2 - \langle T \rangle^2$) plotted as a function of angular scale (multipole ℓ, which roughly corresponds to angular size $180°/\ell$). The baryon density is encoded in the values and particularly the ratios of the peak heights. Reproduced from Reference 60 with permission.

experiments pin down the baryon density. The most recent seven-year WMAP data release gives

$$\eta = (6.19 \pm 0.15) \times 10^{-10} \qquad 11.$$

—a 2.4% measurement!

2.4. Assessing Standard Big Bang Nucleosynthesis: the Lithium Problem(s) Revealed

Prior to WMAP, BBN was the premier means of determining the cosmic baryon density. Standard BBN has one free parameter, η, but three light elements—deuterium, ^{4}He, and ^{7}Li—have well-measured primordial abundances. Thus, the problem is overdetermined: Each element ideally selects a given value of η but, allowing for uncertainties, actually selects a range of η. If the different ranges are concordant, then BBN and cosmology are judged successful, and the cosmic baryon density is measured. This method typically specifies η to within a factor of approximately two (61, 62).

The exquisite precision of the CMB-based cosmic baryon density suggests a new way of assessing BBN (9, 10). We exploit the CMB precision by using η_{WMAP} as an input to BBN. Doing so removes the only free parameter in the standard theory. Propagating errors, we compute likelihoods for all of the light elements. **Figure 5** shows these likelihoods (30), which are based on WMAP data (63). Also shown are measured primordial abundances (discussed above).

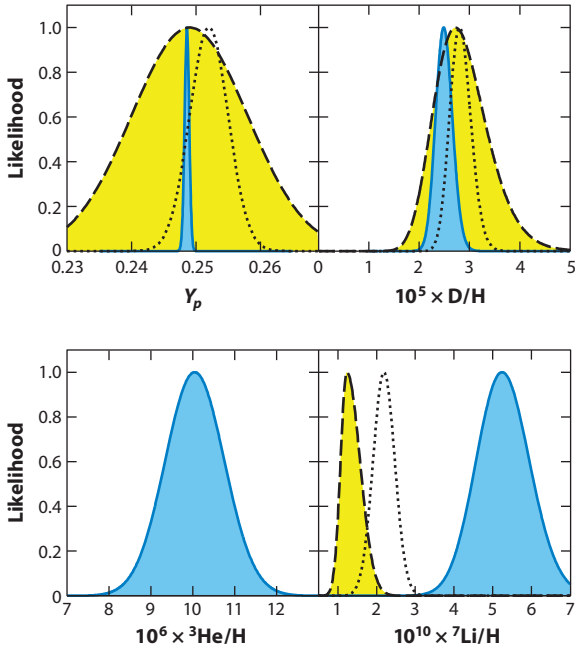

Figure 5

Comparison of big bang nucleosynthesis (BBN)+WMAP predictions and observations. Shown are the likelihood distributions for light-element abundances. The blue curves represent the theory likelihoods predicted for standard BBN through the use of the cosmic baryon density determined by WMAP (63). The yellow curves represent the observational likelihoods based on primordial abundances (see Section 2.2). The dotted curves represent the observational likelihoods for different analyses of abundance data; the difference between these and the yellow curves gives a sense of the systematic errors. Note the spectacular agreement of the ratio of deuterium to hydrogen and, in contrast, the strong mismatch between ^{7}Li theory and data, which constitutes the lithium problem. Reproduced from Reference 30.

Figure 5 shows that deuterium observations are in spectacular agreement with predictions—the likelihoods literally fall on top of one another. This concordance links $z \sim 3$ abundance measurements with $z \sim 10^{10}$ theory and $z \sim 1{,}000$ CMB data, in a quantitative convergence that represents a triumph of the hot big bang cosmology. Also, the ^{4}He predictions are in good agreement with observations, and as noted in Section 2.2, no reliable primordial ^{3}He measurements exist.

Turning to ^{7}Li, the BBN+WMAP predictions and the measured primordial abundance completely disagree: The predictions are substantially higher than the observations. Depending on the treatment of systematic errors in the measured Li/H, the discrepancy is a factor of $\mathrm{Li}_{\mathrm{BBN+WMAP}}/\mathrm{Li}_{\mathrm{obs}} = 2.4\text{–}4.3$, which represents a 4.2–5.3-σ discrepancy. This substantial mismatch constitutes the lithium problem (i.e., the ^{7}Li problem).

Finally, as mentioned in Section 2, standard BBN predicts an unobservable ^{6}Li/H abundance and a ^{6}Li/^{7}Li ratio far below the putative ^{6}Li plateau. To the extent that the ^{6}Li plateau is real, it would constitute a second lithium problem—the so-called ^{6}Li problem. Below, we focus largely on the well-established ^{7}Li problem, but where appropriate we mention the ^{6}Li problem.

3. SOLUTIONS TO THE LITHIUM PROBLEM(S)

The lithium problem was brought into sharp relief with the advent of the WMAP era and has become increasingly acute since then. Possible solutions can be categorized into three groups, according to which part of the preceding analysis is called into question:

1. Astrophysical solutions revise the measured primordial lithium abundance.
2. Nuclear physics solutions alter the reaction flow into and out of mass-7.
3. Solutions beyond the Standard Model invoke new particle physics or nonstandard cosmological physics.

Below, we consider each set of solutions in turn.

3.1. Astrophysical Solutions

First, we consider the possibility that BBN predictions are sound, that is, that standard cosmology and particle physics are correct, and the nuclear physics of mass-7 production is properly calculated. If so, then the measured value of the primordial lithium abundance must be in error. In particular, the true value must be higher by a factor of three to four.

As described in Section 2.2, lithium abundances are measured via absorption lines in the photospheres of primitive, low-metallicity stars. For each star, the lithium line strength is used to infer the Li/H abundance. Lithium abundances are nearly insensitive to metallicity (**Figure 3**)—this Spite plateau implies that lithium is independent of Galactic nucleosynthesis and is primordial, and the plateau level is taken as the primordial abundance. If missteps exist in this chain of reasoning, the lithium problem could be alleviated.

For example, systematic errors could shift Li/H ratios in each star. We seek the total lithium content of the stellar photosphere, that is, the total lithium content summed over all ionization states. However, the single accessible 670.8-nm lithium line is sensitive only to neutral Li^0. Moreover, in the stars of interest, lithium is mostly singly ionized. One must therefore introduce a large ionization correction, $\mathrm{Li}^+/\mathrm{Li}^0$, that is exponentially sensitive to the stellar temperature. Thus, a systematic shift upward in the temperature scale for halo stars would increase all stellar lithium abundances and raise the Spite plateau toward the BBN+WMAP prediction.

In practice, accurate determination of stellar temperatures remains nontrivial because the emergent radiation is not a perfect Planck curve (otherwise, there would be no lithium lines), nor can

local thermodynamic equilibrium be completely attained in the stellar atmospheres. Quantitatively, the needed systematic shift in the temperature scale is approximately $\Delta T_{\rm eff} \simeq 500-600$ K upward, an $\sim$10% increase over fiducial values (outside of previously claimed error bars) (64). A reevaluation of one method to determine stellar temperatures indeed corrects the scale, typically by approximately +200 K (65). However, later, detailed studies of the stellar temperature scale are in good agreement with the fiducial temperature scale, which leaves the lithium problem unresolved (54, 66).

An entirely separate question remains as to whether a star's present lithium content reflects its initial abundance in the star. If the halo stars have destroyed some of their lithium, their present Li/H ratio sets a lower limit to the primordial lithium abundance. Indeed, given the low nuclear binding of ^{7}Li, it need only be exposed to relatively low stellar temperatures ($T \gtrsim 2.5 \times 10^6$ K) to suffer substantial destruction over the many-billion-year life span of a halo star.

Lithium depletion is a major diagnostic of stellar structure and evolution (67–70). For stars of solar composition, lithium destruction (71, 72) has long been studied in stellar evolution models. The major effect is convection, which circulates photospheric material deep into the interior (though still far from the stellar core), where nuclear burning can occur. Models for the evolution of low-metallicity stars, appropriate for the Spite plateau, now include numerous mixing effects that can change the photospheric lithium: convective motions, turbulence, rotational circulation, diffusion and gravitational settling, and internal gravity waves (70, 73–75). These effects must occur at some level, and models have had some success in fitting certain observed trends in halo stars. There is general agreement that for stars with low metallicities, convective zones are substantially shallower than in solar-metallicity stars, so depletion should be much smaller than the factor of $\sim 10^2$ observed in the Sun (76). However, it remains difficult for models to quantitatively fit all of the data (49).

Thus observational efforts to find clues for lithium depletion in the Spite plateau stellar data remain extremely important. One study found the Spite plateau in field halo stars to be very thin, with no detectable star-to-star variations around the Li/Fe trend; this observation revealed a small positive slope in Li/H versus Fe/H (48). A small lithium increase with metallicity is required due to contamination from Galactic cosmic-ray production of ^{7}Li and ^{6}Li (57). An analysis of lithium and iron abundances in stars from the same globular cluster found trends consistent with lithium depletion via diffusion and turbulent mixing; some models suggest that these effects could remove the lithium problem entirely (50). However, systematic differences between globular cluster and field star lithium abundances raise concern about globular clusters at sites for constraining primordial lithium (56).

Recently, several groups found that at very low metallicity, [Fe/H] $\lesssim -3$, lithium abundances, on average, fall below the Spite plateau (i.e., below the levels observed at metallicities $-3 \lesssim$ [Fe/H] $\lesssim -1.5$) (51–53, 55). These groups also found that the star-to-star scatter in Li/H becomes significant below [Fe/H] $\lesssim -3$. This finding appears to confirm the presence of significant lithium depletion in at least some halo stars.

The recent evidence for lithium depletion at very low metallicities is a major development, but its implications for primordial lithium remain unclear. No significant scatter is detected in plateau stars with $-3 \lesssim$ [Fe/H] $\lesssim -1.5$. Also, in no stars is Li/H observed above the plateau, and in no metal-poor stars is Li/H near the WMAP+BBN value. Finally, although ^{6}Li measurements are difficult and controversial, there is general agreement that ^{6}Li is present in at least some plateau stars. This much more fragile isotope strongly constrains thermonuclear burning processes—if stellar material is exposed to temperatures hot enough to significantly reduce ^{7}Li, then ^{6}Li should be completely destroyed (77).

Determination of the primordial lithium abundance continues to be the focus of rapid progress. However, the observational status of primordial lithium remains unsettled. On the one hand, a

purely astrophysical solution to the lithium problem remains possible. On the other hand, the observed lithium trends—particularly the small lithium scatter in temperature and metallicity and the presence of ^{6}Li—strongly constrain (but do not rule out) such solutions. Consequently, it is entirely possible that the lithium problem cannot be resolved astrophysically. We must therefore seek other explanations of the discrepancy; we discuss these explanations below.

3.2. Nuclear Physics Solutions

Consider the possibility that the measured primordial lithium abundance is correct and that the Standard Model of particle physics and the standard cosmology are also sound. In this case, the lithium problem must point to errors in the BBN light-element predictions, in the form of incorrect implementation of standard cosmological and/or Standard Model physics.

However, the standard BBN calculation is very robust and thus difficult to perturb. As summarized in Section 2, standard BBN rests on very well determined physics applied in a very simple system. The cosmological framework of BBN is that of a homogeneous universe [guaranteed by the smallness of the observed CMB temperature fluctuations (3)], with a cosmic expansion governed by exact expressions in general relativity. The microphysics is that of the Standard Model, which is also very well determined. The relativistic species, which constitute cosmic radiation that dominates the energy density, are very well thermalized, and thus their properties are those of Bose-Einstein and Fermi-Dirac gases, for which exact expressions are also available.

The weak and strong (i.e., nuclear) interactions are also well grounded in theory and are calibrated empirically, but for BBN the needed physics is complicated (nuclear networks are large) and lies the farthest from first principles. Thus, these are the only possible weak links in the standard BBN calculation, and it is here that solutions to the lithium problem have been sought.

3.2.1. New and revised reactions. One possibility is that weak and nuclear reactions in the BBN calculations have been miscalculated due to reactions that are entirely missing or that are included but have incorrect rates. However, as described in Section 2 and shown in **Figure 1**, only a relatively small number of reactions are important for producing the light elements, and all of them have been measured in the laboratory at the relevant energies. Their uncertainties have also been calculated and propagated through the BBN code and are folded into the likelihoods shown in **Figure 5**. Moreover, BBN calculations use a much more extended reaction network than depicted in **Figure 1**; all the initial-state pairings of $A \leq 7$ species are present but, in practice, most are unimportant (23, 78–83). Thus, to change the primordial lithium predictions requires surprises of some kind—either (*a*) the cross sections of the known important reactions have uncertainties far beyond the quoted errors, or (*b*) the cross sections for normally unimportant reactions have been vastly underestimated.

For the important reactions shown in **Figure 1**, mass-7 production is dominated by the single reaction ^{3}He$(\alpha, \gamma)^7$Be. Although the quoted error budget in the measured cross section is small, ~5% (84), absolute cross sections are difficult to measure. However, this reaction is also crucial in the production of solar neutrinos. To fix the cosmic lithium problem, the ^{3}He$(\alpha, \gamma)^7$Be normalization would need to be lower by a factor of three to four; if this were the case, the ^{7}Be and ^{8}B solar neutrino fluxes would be lower by a similar factor. Thus, we can view the Sun as a reactor that probes the ^{3}He$(\alpha, \gamma)^7$Be rate, and the spectacular and precise agreement between solar neutrino predictions and observations then becomes a measurement of the rate normalization, which confirms the experimental results and removes this scenario as a solution to the lithium problem (85).

Weak rates in BBN have received a great deal of attention (86–94). The basic $n \leftrightarrow p$ interchange rates (Equation 4) are most accurately normalized to the neutron lifetime. Corrections to the

tree-level rates have $\lesssim$1% effects on abundances and, thus, are far too small to impact the lithium problem (94).

Corrections to the standard thermonuclear rates have also been considered. The effects of nonthermal daughter particles has been studied and found to be negligible (82, 95). Plasma effects and electron Coulomb screening are also unimportant (96).

Turning to (normally) subdominant reactions, Angulo et al. (97) noted that the (nonresonant) cross section for ^{7}Be(d, α)αp was poorly determined and could solve the lithium problem if it were larger by a factor of $\sim$100. These authors measured the cross section at BBN energies but found values that were a factor of $\sim$10 *smaller* than had been used previously.

Finally, the possibility of entirely new reactions was recently studied by Boyd et al. (82). These authors systematically considered a large set of reactions, some of which had been neglected in prior calculations. The focus of this study was almost exclusively on nonresonant reactions, so even when extremely large systematic uncertainties in known cross sections are allowed for, most new channels remain unimportant. The loophole in this analysis is the presence of new or poorly measured resonances.

3.2.2. Resonances. Both standard and nonstandard reaction pathways to primordial mass-7 are firmly anchored to experimental data. The only remaining new nuclear physics can intervene only via resonances that have evaded experimental detection or whose effects have been underestimated. Cyburt & Pospelov (98) point out that the production of the known resonance $^7\mathrm{Be} + d \rightarrow {}^9\mathrm{B}^*(16.71\,\mathrm{MeV})$ (**Figure 1**) is poorly constrained experimentally. Within current uncertainties, this resonance could promote the $^7\mathrm{Be} + d$ channel to become the dominant ^{7}Be destruction mode, which would solve the lithium problem in an elegant manner.

Generalizing the Cyburt & Pospelov (98) suggestion, the authors of Reference 99 searched the entire resonance solution space for BBN. They systematically considered all the compound states created in mass-7 destruction via all possible two-body reactions of the form (n, p, d, t, ^{3}He, ^{4}He)+(^{7}Li, ^{7}Be). Most possibilities were found to be unimportant. However, in addition to the $^7\mathrm{Be} + d \rightarrow {}^9\mathrm{B}^*(16.71\,\mathrm{MeV})$ resonance, two other potentially important states were identified (**Figure 1**). On the one hand, the $^7\mathrm{Be} + t \rightarrow {}^{10}\mathrm{B}^*(18.80\,\mathrm{MeV})$ resonance is known and, within present uncertainties, could be significant. On the other hand, there are few data on high-lying states of ^{10}C, but if a $^{10}\mathrm{C}^*(15.0\,\mathrm{MeV})$ exists and has $J^\pi = 1^-$ or 2^-, it also could bring cosmic lithium into concordance if the reaction widths are large enough. This last possibility would be a homage to Hoyle's (99) celebrated prediction of the $^{12}\mathrm{C}^*$ (7.65 MeV) state, which solved the so-called carbon problem of stellar nucleosynthesis.

Any or all of these states could solve the lithium problem, but only if they have very large widths. This in turn requires rather large channel radii (>10 fm). To find such high values would be unusual but, nevertheless, would be a much less dramatic surprise than the discovery of new physics, as discussed in the next section.

Fortunately, all of these states are experimentally accessible. To identify or exclude them marks the endgame for a nuclear solution to the lithium problem.

3.3. Solutions Beyond the Standard Model

Finally, we discuss the most radical class of solutions to the lithium problem. Specifically, we assume that primordial lithium has been correctly measured and that the nuclear physics of BBN has been calculated correctly and holds no surprises. In this case, we are forced to question the assumptions underlying the standard BBN calculation; that is, we must go beyond the Standard

Model of particle physics and/or the standard cosmology. For details beyond the overview below, see References 15 and 16.

3.3.1. Dark matter decay and supersymmetry. The existence of dark matter is now well established, and its cosmic abundance has been inferred precisely; for recent reviews, see References 100–102. If dark matter takes the form of a relic particle created in the very early universe, it must be nonbaryonic. No Standard Model particles have the right properties, and thus dark matter demands physics beyond the Standard Model. Dark matter must of course be present during BBN. Ordinarily, it is assumed to be both nonrelativistic and weakly interacting and, hence, unimportant to cosmic dynamics and microphysical interactions. Similarly, dark energy is assumed to be negligible.

Although the identity of the dark matter is unknown, a simple, popular, and physically well-motivated possibility is that dark matter today consists of relic weakly interacting massive particles (WIMPs). In particular, if the universe begins with equal abundances of WIMPs and anti-WIMPs (or if WIMPs are their own antiparticles), then their abundance is determined by the freeze-out of their annihilations. To reproduce $\Omega_m \simeq 0.3$ today, the annihilations must occur at ~TeV scales (well before BBN). By happy accident, this is also the scale of the weak interaction and of current accelerator experiments. This coincidence is termed the WIMP miracle (100–102).

WIMPs today are probably the stable end points of a decay cascade. If so, then the WIMPs are the daughters born in the decays of the next-lightest particles in the cascade. The nature of these decays is model dependent, but they generally produce Standard Model particles that interact with the background plasma. If the decays occur during or after BBN, the interactions can change light-element abundances (103–116) and therefore could solve the lithium problem(s) (32, 117–123).

We thus examine the effects of decaying massive particles during or after BBN. Consider a particle X (and $\bar{X}$, if they are distinct) with mass $m_X \gg m_p$, which decays with lifetime τ_X. The decays can have electromagnetic and/or hadronic channels, and given the massive nature of X, such decay products will be very relativistic and thus nonthermal.

As these electromagnetic and/or hadronic cascades thermalize in the cosmic environment, they interact with the light elements largely via fragmentation (photodissociation or spallation). For example, high-energy nucleons, N, fragment ^{4}He:

$$N + {}^4\mathrm{He} \rightarrow \begin{cases} 2n + 2p + N \\ d + d + N \\ d + {}^3\mathrm{A} \\ \cdots \end{cases} . \qquad 12.$$

This process reduces the ^{4}He abundance but, more importantly, creates new deuterium and ^{3}He. Furthermore, the secondary particles shown in Equation 12 are themselves nonthermal and can initiate further interactions with the background thermal light nuclides. Of particular importance is the conversion of ^{7}Be into ^{7}Li with secondary neutrons,

$$n + {}^7\mathrm{Be} \rightarrow p + {}^7\mathrm{Li}, \qquad 13.$$

which substantially enhances mass-7 destruction because of the lower Coulomb barrier for ^{7}Li. Also of interest is the nonthermal production of ^{6}Li via secondary nonthermal deuterons,

$$d + {}^4\mathrm{He} \rightarrow {}^6\mathrm{Li} + \gamma. \qquad 14.$$

Clearly, both processes are of great interest for both lithium problems.

Figure 6 shows light-element abundances in the presence of a hadronically decaying particle X. Abundance contours are plotted as a function of decay lifetime τ_X, and the predecay X

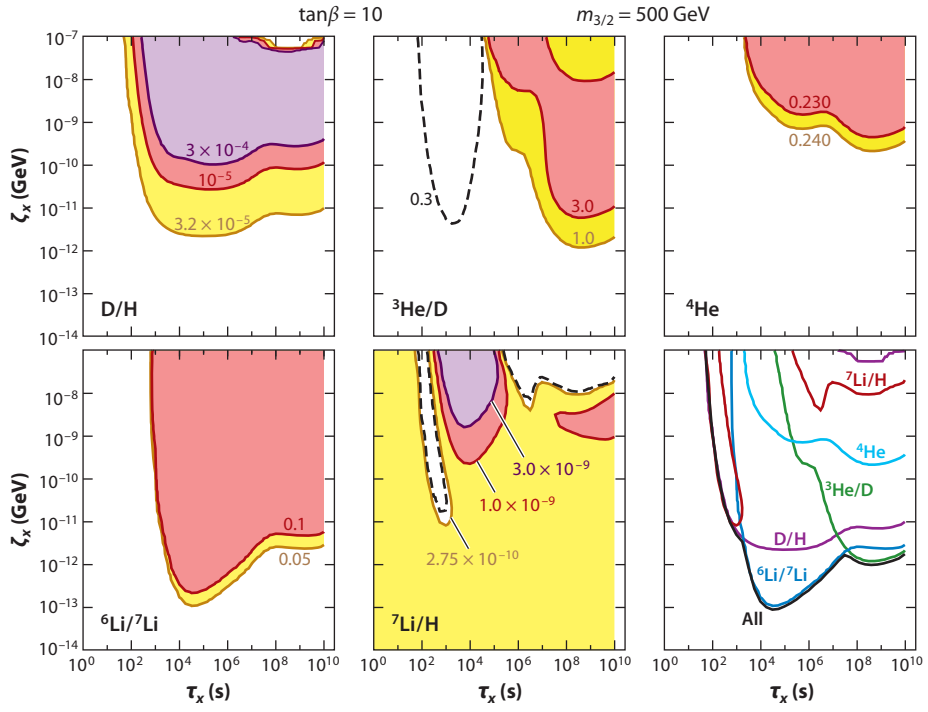

Figure 6

Effect of nonthermal particle injection on light-element abundances. The colored areas indicate parameter regions in which the predicted light-element abundances disagree with observations, and the remaining, white regions are allowed. Each panel shows abundance contours in the presence of the hadronic decay of a (neutral) particle X, plotted as a function of X abundance ζ_X (Equation 15) and mean life τ_X. Results are shown for a hadronic branching ratio $B_h = 1$. As summarized in the bottom right panel, the parameter regions in which the ^{7}Li problem is solved also lead to deuterium production, thereby placing the two in tension. Reproduced from Reference 31.

abundance is

$$\zeta_X \equiv \frac{m_X n_X}{n_\gamma} = m_X \frac{n_X}{n_b} \eta. \qquad 15.$$

In the absence of X decays, cosmic expansion dilutes baryons and X particles in the same way, so ζ_X remains constant. **Figure 6** adopts a hadronic branching fraction $B_h = 1$; that is, all the decays produce hadrons.

As shown in **Figure 6**, at fixed τ_X, the light-element perturbation is proportional to the X abundance. The limit $\zeta_X \to 0$ lies at the bottom of the plot and corresponds to the unperturbed (standard BBN) case. At fixed abundance ζ_X, the light-element effects strongly depend on particle lifetime, which determines when the light elements are perturbed. For example, at $\tau_X \lesssim 10$ s, decays occur before the light elements are formed, so the light elements are unaffected. Hadronic decays dominate the perturbations in the $\tau_X \lesssim 10^6$ s region of greatest interest; electromagnetic decays dominate at longer times.

In the ^{7}Li/H panel of **Figure 6**, the colored regions include the unperturbed low-ζ_X regime, reflecting the lithium problem for standard BBN. However, for a relatively narrow region with lifetimes $\tau_X \sim 10^2$–10^3 s, the ^{7}Li abundance is reduced and brought into accord with observation. This reduction arises from the production of secondary neutrons (Equation 12), which facilitate

mass-7 destruction via ^{7}Be-to-^{7}Li conversion (Equation 13); at longer lifetimes, the secondary neutrons decay. For 10^2–10^3 s lifetimes to be viable, however, the other light elements must remain in concordance. As shown in the bottom right panel, in the regime in which ^{7}Li is reduced, all other constraints are satisfied except for D/H, which is unacceptably high due to secondary deuteron production. This tension between deuterium and ^{7}Li is a fundamental feature of decay scenarios, and it may allow for solutions but requires fine tuning.

Supersymmetry provides well-motivated candidates for decaying dark matter (124–126). Supersymmetry doubles the particle content of nature by requiring opposite-statistics (fermion ↔ boson) partners for every known fundamental particle. These partners are copiously produced in the very early universe. The lightest supersymmetric partner (LSP) is the stable end product of the decays of higher-mass supersymmetric particles, so naturally it becomes a dark matter candidate (127, 128). These decays are a fundamental aspect of supersymmetric dark matter, and thus supersymmetric scenarios demand that particle decays occur. Moreover, even in the simplest scenarios—namely the constrained minimal supersymmetric Standard Model—the lifetime of the next-to-lightest supersymmetric partner can be long: $\gtrsim$100 s. Thus, minimal supersymmetry has the tantalizing potential to solve the lithium problem.

Figure 7 illustrates the interplay between supersymmetry and the lithium problem (32). The context is minimal supersymmetry, in which the spin-$\frac{3}{2}$ gravitino is the next-to-lightest supersymmetric partner; it decays into the LSP neutralino that today constitutes dark matter. For a benchmark scenario in this model, the superpartner mass spectrum, lifetimes, and decay products are calculated. These are used to compute light-element abundances, with nuclear uncertainties propagated; the results are compared with observations. The resulting χ^2 is plotted as a function of gravitino mass $m_{3/2}$ and predecay abundance $\zeta_{3/2}$. At low $\zeta_{3/2}$, we recover the unperturbed, standard case, where $\chi^2 \approx 32$ for one effective degree of freedom (three light elements minus two

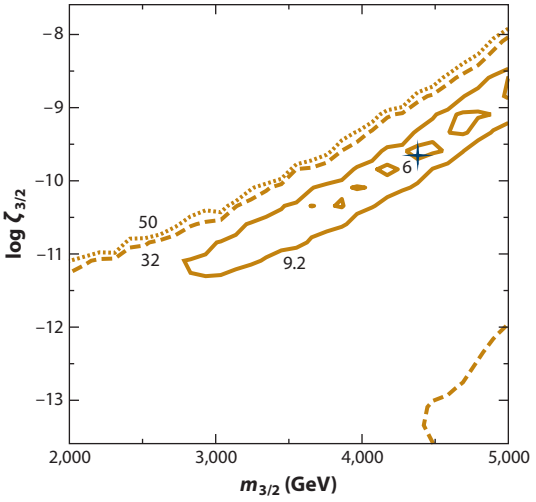

Figure 7

Light-element constraints on gravitino decays in the context of the constrained minimal supersymmetric Standard Model. Shown are χ^2 contours based on light-element abundance constraints and one effective degree of freedom, over the space of gravitino mass $m_{3/2}$ and abundance $\zeta_{3/2}$ (Equation 15). The cross indicates the maximum χ^2. The diagonal "archipelago" shows the region in which the lithium problem is greatly reduced by trading off ^{7}Li destruction for some degree of deuterium production. Reproduced from Reference 32.

parameters)—a poor fit. At high $\zeta_{3/2}$, the light-element perturbations are worsened over the standard case, and these supersymmetric parameters are excluded by BBN. Most interestingly, along the diagonal loop, the fit improves, and in the interior "islands," χ^2 drops below six, which corresponds to $\sim 2.4\,\sigma$. This region shows substantial improvement over standard BBN and physically arises as the regime of optimal trade-off between ^{7}Li destruction and deuterium production. This region is therefore a possible supersymmetric solution to the lithium problem, albeit statistically marginal and fine-tuned.

Finally, an entirely new aspect of decaying dark matter alteration of BBN has recently emerged. If the decaying particles are electrically charged, then the negatively charged dark matter can form bound states with charged nuclei, such as (pX^-), (^{4}HeX^-), and (^{7}BeX^-). As discussed by Pospelov (116), these bound states unleash a wide array of new effects, in addition to the perturbations accompanying X^- decays. For the heavy X^- of interest, the binding energy of ($^{\mathrm{A}}_{\mathrm{Z}}X^-$) is $B = \mathrm{Z}^2\mathrm{A}\alpha^2 m_p/2 \approx 30\mathrm{Z}^2\mathrm{A}$ keV, comparable to nuclear binding. The Bohr radius is $a = (2\alpha\mathrm{ZA}m_p)^{-1} \approx 1\mathrm{A}^{-1}\mathrm{Z}^{-1}$ fm, comparable to nuclear sizes. Bound-state Coulomb barriers are thus reduced, and (^{7}BeX^-) becomes easier to destroy.

Beyond these basic effects, a new bound-state chemistry can occur; its nature is still being actively studied. An important effect (116) is catalysis, particularly $d + (^4\mathrm{He}X) \rightarrow {}^6\mathrm{Li} + X$, which enhances ^{6}Li production far above the ordinarily small radiative capture $d(\alpha, \gamma)^6$Li. This enhancement can be orders of magnitude, which may address the ^{6}Li problem, if real, but often overproduces ^{6}Li. Rates for catalyzed reactions have recently been calculated to high precision (129). Intriguingly, (^{8}BeX^-) states have a binding energy very close to that for the $^8\mathrm{Be} \rightarrow aa$ breakup; if the binding energy is larger, then (^{8}BeX^-) is stable and can allow for cosmological production of ^{9}Be (121, 130).

The general properties of X^- recombination and bound states, and their impact on BBN, were studied in References 15, 116, 121, 122, 131, and 132. If we consider the bound-state effect alone (i.e., ignoring decay effects), catalyzed ^{7}Be destruction is effective and catalyzed ^{6}Li is not overproduced for a sufficiently large X^- abundance in the regime $\tau_X \sim 2{,}000$ s (131). Indeed, there are regions of parameter space wherein both the ^{7}Li and ^{7}Li problems are solved. A full calculation of bound-state and decay effects together is required to verify whether solutions remain in specific detailed models; early calculations confirm that solution space exists around $\tau_X \sim 10^3$ (122, 133).

Catalyzed production of ^{9}Be also occurs and is constrained by the nonobservation of a beryllium Spite plateau; the resulting limits on τ_X are comparable to those imposed by limits on primordial ^{6}Li (121). ^{9}Be constraints have the added advantage of relying on elemental abundances, which are much simpler to reliably obtain than isotopic abundances are. However, ^{9}Be was recently investigated by use of updated catalysis rates (129), which greatly reduce the ^{9}Be production rate. The resulting ^{9}Be abundance is quite small, below observable levels (130).

Bound-state effects are important in the context of minimal supersymmetry. There exists substantial parameter space in which the gravitino is the LSP and thus the dark matter, and the next-to-lightest supersymmetric partner is the charged stau $\tilde{\tau}^{\pm}$, the scalar partner to the tau lepton. Such models are probed by bound-state BBN, which imposes constraints that are complementary to accelerator limits (120, 121, 123, 131–135). The solutions to the ^{7}Li problem, and possibly also the ^{6}Li problem, that exist at $\tau_X \sim 1{,}000$ s could be interpreted as support for these models.

Decaying dark matter scenarios introduce a rich array of novel processes that can alter light elements during and after BBN. Moreover, such scenarios have a well-motivated origin in supersymmetric cosmologies. Indeed, decaying-particle BBN offers important constraints on supersymmetry. Furthermore, the ^{7}Li problem, and possibly also the ^{6}Li problem, can be solved in decaying particle scenarios that are realized in plausible minimal supersymmetric

scenarios. This area of research is ripe for further theoretical, observational, and experimental development.

3.3.2. Changing fundamental constants. Observations of multiple atomic transitions in metals residing in high-redshift quasar absorption systems test fundamental physics in environments that lie at great space-time separations from our own; for a review, see Reference 136. Surprisingly, some data hint at variations in the fine-structure constant at $z \sim 3$, showing $\delta\alpha_{\rm EM}/\alpha_{\rm EM} \simeq -0.5 \times 10^{-5}$ at the $\sim$5-σ level, whereas others are consistent, with no variation. Thus, the observational situation remains unsettled but intriguing.

Time variations in low-energy physics can be accommodated and are even expected in the context of some unified theories that generally predict stronger variations at earlier times. Moreover, an underlying unified theory implies that all Standard Model couplings and particle masses should vary, with definite but model-dependent interrelationships.

There is theoretical impetus, and some observational motivation, to contemplate changes in fundamental constants during BBN. The change in light elements depends on which parameters (e.g., couplings and masses) evolve, as well as on the size of the perturbations (137–141). In general, there is large model dependence in quantifying these variations, the links among them, and their manifestation in nuclear properties (e.g., masses, binding energies, and cross sections).

An alternative approach is to consider the BBN implications of variation in nuclear physics parameters (142, 143). Coc et al. (139) systematically studied the light-element response to variations in $\alpha_{\rm EM}$, the electron mass m_e, the neutron lifetime τ_n, the neutron-proton mass difference $m_n - m_p$, and the deuteron-binding energy B_D. The most sensitive of these parameters is the deuteron-binding energy. A change of $-0.075 \lesssim \delta B_D/B_D \lesssim -0.04$ lowers the ^{7}Li abundance into concordance without perturbing ^{4}He or D/H beyond their observed error range. Thus, unified models that predict changes of this order could solve the lithium problem.

3.3.3. Nonstandard cosmologies. The lithium problem could indicate nonstandard cosmology rather than nonstandard particle physics. One recent such proposal is that cosmic acceleration could result from large-scale inhomogeneities in the cosmic density. Isotropy constraints can be satisfied if we occupy a privileged view from near the center of a spherically symmetric cosmic underdensity, which returns to the cosmic mean only at horizon-scale distances (144). Such a scenario explains cosmic acceleration within general relativity—and without invoking dark energy—but it must abandon the cosmological principle, instead requiring that ours be a privileged view of the universe.

Aesthetics aside, observations probe such an inhomogeneous cosmos. BBN can occur differently in such a universe, if the baryon-to-photon ratio varies along the inhomogeneity. In particular, Regis & Clarkson (145) emphasize that the observations of ^{7}Li are made locally, at low z, whereas both D/H and the CMB are measured in the distant universe at high z. If the local baryon-to-photon ratio η_0 is lower by a factor of approximately two, then indeed one would expect (*a*) local ^{7}Li to fall below the WMAP prediction and (*b*) D/H to agree.

This clever scenario must face an array of observational tests. Relaxed galaxy clusters probe the cosmic baryon-to-matter fraction and show variations of $\lesssim$8% out to $z \sim 1$, far less than the $\sim$50% variation needed for lithium abundances (146). Moreover, local measurements of D/H even more directly constrain the local η measurement. Because some stellar destruction may well have occurred, the local D/H sets a lower limit on the primordial abundance. In the lower halo of our own Galaxy, D/H $= (2.31 \pm 0.24) \times 10^{-5}$. This value is in good agreement with the high-z D/H measurements and the WMAP+BBN predictions; it is therefore inconsistent with the low η needed for a low local ^{7}Li/H.

Other nonstandard cosmology scenarios have been proposed to solve the lithium problem. One such scenario suggests that a large fraction (approximately one-third to one-half) of baryons were processed through the first generation of stars (Population III), which ejected lithium-free matter (147). Such models face great difficulties because of the substantial D/H depletion and ^{3}He production that must also occur (148, 149).

4. DISCUSSION AND OUTLOOK

BBN has entered the age of precision cosmology. This transition has brought success in the spectacular agreement between high-redshift deuterium and the BBN+WMAP prediction, as well as in the WMAP confirmation of the long-standing BBN prediction of nonbaryonic dark matter. However, this new precision has raised new questions: The measured primordial ^{7}Li abundance falls persistently and significantly below BBN+WMAP predictions. Moreover, there are controversial hints of a primordial ^{6}Li abundance that is orders of magnitude above the standard prediction.

As discussed above, there are disparate explanations for the lithium problem(s). Fortunately, most of them will become testable in the near future. These potential explanations include the following.

1. Astronomical observations. Recent indications of lithium depletion in extremely metal-poor halo stars are tantalizing. In the coming era of large, deep sky surveys such as LSST, we may expect that many more such stars will be identified and that the lithium trends will be explored in large statistical samples, which will require careful comparison with theory. Observations of ^{6}Li remain challenging, and it remains unclear what trends exist with metallicity. Great insight would result from alternative measures of primordial lithium, for instance, in the interstellar medium of metal-poor galaxies nearby or at high redshift.
2. Nuclear experiments. The enormous effort of the nuclear community has empirically pinned down nearly all nuclear inputs to BBN. Remaining are a few known or proposed resonances that would amplify ^{7}Be destruction. These resonances are within the reach of present facilities, so the nuclear physics of standard BBN can and will be fully tested.
3. Collider and dark matter experiments. The LHC is operational, and much of minimal supersymmetry lies within its reach. The discovery of supersymmetry would revolutionize particle physics and cosmology and would transform decaying particle BBN scenarios into canonical early universe cosmology. Alternatively, if the LHC fails to find supersymmetry and/or finds surprises of some other kind, it will represent a paradigm shift for particle physics and particle cosmology, and BBN will lie at the heart of this transformation.

DISCLOSURE STATEMENT

The author is not aware of any affiliations, memberships, funding, or financial holdings that might be perceived as affecting the objectivity of this review.

ACKNOWLEDGMENTS

It is a pleasure to thank my collaborators in primordial nucleosynthesis and closely related areas: Nachiketa Chakraborty, Richard Cyburt, John Ellis, Feng Luo, Keith Olive, Tijana Prodanović, Evan Skillman, Vassilis Spanos, and Gary Steigman. I am particularly grateful to Keith Olive for comments on an earlier version of this review.

LITERATURE CITED

1. Wagoner RV, Fowler WA, Hoyle F. *Astrophys. J.* 148:3 (1967)
2. Steigman G. *Annu. Rev. Nucl. Part. Sci.* 57:463 (2007)
3. Spergel DN, et al. *Astrophys. J. Suppl.* 148:175 (2003)
4. Larson D, et al. *Astrophys. J. Suppl.* 192:16 (2011)
5. Riess AG, et al. *Astron. J.* 116:1009 (1998)
6. Perlmutter S, et al. *Astrophys. J.* 517:565 (1999)
7. Tonry JL, et al. *Astrophys. J.* 594:1 (2003)
8. Wood-Vasey WM, et al. *Astrophys. J.* 666:694 (2007)
9. Schramm DN, Turner MS. *Rev. Mod. Phys.* 70:303 (1998)
10. Cyburt RH, Fields BD, Olive KA. *Astropart. Phys.* 17:87 (2002)
11. Cyburt RH, Fields BD, Olive KA. *Phys. Lett.* B567:227 (2003)
12. Cyburt RH. *Phys. Rev. D* 70:023505 (2004)
13. Coc A, et al. *Astrophys. J.* 600:544 (2004)
14. Cuoco A, et al. *Int. J. Mod. Phys. A* 19:4431 (2004)
15. Pospelov M, Pradler J. *Annu. Rev. Nucl. Part. Sci.* 60:539 (2010)
16. Jedamzik K, Pospelov M. *New J. Phys.* 11:105028 (2009)
17. Iocco F, et al. *Phys. Rep.* 472:1 (2009)
18. Krauss LM, Romanelli P. *Astrophys. J.* 358:47 (1990)
19. Smith MS, Kawano LH, Malaney RA. *Astrophys. J. Suppl.* 85:219 (1993)
20. Fiorentini G, Lisi E, Sarkar S, Villante FL. *Phys. Rev. D* 58:063506 (1998)
21. Hata N, et al. *Phys. Rev. Lett.* 75:3977 (1995)
22. Nollett KM, Burles S. *Phys. Rev. D* 61:123505 (2000)
23. Cyburt RH, Fields BD, Olive KA. *New Astron.* 6:215 (2001)
24. Coc A, et al. *Astrophys. J.* 600:544 (2004)
25. Descouvemont P, et al. *At. Data Nucl. Data Tables* 88:203 (2004)
26. Serpico PD, et al. *J. Cosmol. Astropart. Phys.* 12:10 (2004)
27. Khatri R, Sunyaev RA. arXiv:1009.3932 [astro-ph.CO] (2010)
28. Thomas D, Schramm DN, Olive KA, Fields BD. *Astrophys. J.* 406:569 (1993)
29. Vangioni-Flam E, et al. *New Astron.* 4:245 (1999)
30. Cyburt RH, Fields BD, Olive KA. *J. Cosmol. Astropart. Phys.* 11:12 (2008)
31. Cyburt RH, et al. *J. Cosmol. Astropart. Phys.* 10:21 (2009)
32. Cyburt RH, et al. *J. Cosmol. Astropart. Phys.* 10:32 (2010)
33. Burles S, Tytler D. *Astrophys. J.* 507:732 (1998)
34. Burles S, Tytler D. *Astrophys. J.* 499:699 (1998)
35. O'Meara JM, et al. *Astrophys. J.* 552:718 (2001)
36. Kirkman D, et al. *Astrophys. J. Suppl.* 149:1 (2003)
37. O'Meara JM, et al. *Astrophys. J. Lett.* 649:L61 (2006)
38. Pettini M, et al. *Mon. Not. R. Astron. Soc.* 391:1499(2008)
39. Olive KA, Skillman ED. *New Astron.* 6:119 (2001)
40. Olive KA, Skillman ED. *Astrophys. J.* 617:29 (2004)
41. Peimbert A, Peimbert M, Luridiana V. *Astrophys. J.* 565:668 (2002)
42. Izotov YI, Thuan TX. *Astrophys. J.* 500:188 (1998)
43. Izotov YI, Thuan TX. *Astrophys. J.* 602:200 (2004)
44. Bania TM, Rood RT, Balser DS. *Space Sci. Rev.* 130:53 (2007)
45. Vangioni-Flam E, Olive KA, Fields BD, Casse M. *Astrophys. J.* 585:611 (2003)
46. Asplund M, et al. *Astrophys. J.* 644:229 (2006)
47. Spite F, Spite M. *Astron. Astrophys.* 115:357 (1982)
48. Ryan SG, Norris JE, Beers TC. *Astrophys. J.* 523:654 (1999)
49. Bonifacio P, et al. *Astron. Astrophys.* 462:851 (2007)
50. Korn AJ, et al. *Nature* 442:657 (2006)
51. Sbordone L, et al. *Astron. Astrophys.* 522:A26 (2010)

52. Aoki W, et al. *Astrophys. J.* 698:1803 (2009)
53. Hosford A, et al. *Astron. Astrophys.* 493:601 (2009)
54. Hosford A, et al. *Astron. Astrophys.* 511:A47 (2010)
55. Meléndez J, et al. *Astron. Astrophys.* 515:L3 (2010)
56. González Hernández JI, et al. *Astron. Astrophys.* 505:L13 (2009)
57. Ryan SG, et al. *Astrophys. J. Lett.* 530:L57 (2000)
58. Monaco L, et al. *Astron. Astrophys.* 519:L3 (2010)
59. Cayrel R, et al. *Astron. Astrophys.* 473:L37 (2007)
60. Hu W, Dodelson S. *Annu. Rev. Astron. Astrophys.* 40:171 (2002)
61. Yang J, et al. *Astrophys. J.* 281:493 (1984)
62. Walker TP, et al. *Astrophys. J.* 376:51 (1991)
63. Komatsu E, et al. *Astrophys. J. Suppl.* 180:330 (2009)
64. Fields BD, Olive KA, Vangioni-Flam E. *Astrophys. J.* 623:1083 (2005)
65. Meléndez J, Ramírez I. *Astrophys. J. Lett.* 615:L33 (2004)
66. Casagrande L, et al. *Astron. Astrophys.* 512:A54 (2010)
67. Wallerstein G, Conti PS. *Annu. Rev. Astron. Astrophys.* 7:99 (1969)
68. Spite M, Spite F. *Annu. Rev. Astron. Astrophys.* 23:225 (1985)
69. Gustafsson B. *Annu. Rev. Astron. Astrophys.* 27:701 (1989)
70. Pinsonneault M. *Annu. Rev. Astron. Astrophys.* 35:557 (1997)
71. Bodenheimer P. *Astrophys. J.* 142:451 (1965)
72. Iben I Jr. *Astrophys. J.* 147:624 (1967)
73. Pinsonneault MH, Deliyannis CP, Demarque P. *Astrophys. J. Suppl.* 78:179 (1992)
74. Talon S, Charbonnel C. *Astron. Astrophys.* 418:1051 (2004)
75. Richard O, Michaud G, Richer J. *Astrophys. J.* 619:538 (2005)
76. Greenstein JL, Richardson RS. *Astrophys. J.* 113:536 (1951)
77. Brown L, Schramm DN. *Astrophys. J. Lett.* 329:L103 (1988)
78. Malaney RA, Fowler WA. *Astrophys. J. Lett.* 345:L5 (1989)
79. Thomas D, et al. *Astrophys. J.* 430:291 (1994)
80. Iocco F, et al. *Phys. Rev. D* 75:087304 (2007)
81. Vangioni-Flam E, Coc A, Casse M. *Astron. Astrophys.* 360:15 (2000)
82. Boyd RN, Brune CR, Fuller GM, Smith CJ. *Phys. Rev. D* 82:105005 (2010)
83. Chakraborty N, Fields BD, Olive KA. *Phys. Rev. D* 83:063006 (2011)
84. Adelberger EG, et al. *Rev. Mod. Phys.* In press (2011)
85. Cyburt RH, Fields BD, Olive KA. *Phys. Rev. D* 69:123519 (2004)
86. Dicus DA, et al. *Phys. Rev. D* 26:2694 (1982)
87. Seckel D. arXiv:hep-ph/9305311 (1993)
88. Dolgov AD, Fukugita M. *Phys. Rev. D* 46:5378 (1992)
89. Kernan PJ, Krauss LM. *Phys. Rev. Lett.* 72:3309 (1994)
90. Dodelson S, Turner MS. *Phys. Rev. D* 46:3372 (1992)
91. Hannestad S, Madsen J. *Phys. Rev. D* 52:1764 (1995)
92. Lopez RE, Turner MS. *Phys. Rev. D* 59:103502 (1999)
93. Esposito S, Mangano G, Miele G, Pisanti O. *Nucl. Phys. B* 540:3 (1999)
94. Smith CJ, Fuller GM. *Phys. Rev. D* 81:065027 (2010)
95. Voronchev VT, Nakao Y, Nakamura M. *Astrophys. J.* 725:242 (2010)
96. Itoh N, Nishikawa A, Nozawa S, Kohyama Y. *Astrophys. J.* 488:507 (1997)
97. Angulo C, et al. *Astrophys. J. Lett.* 630:L105 (2005)
98. Cyburt RH, Pospelov M. arXiv:0906.4373 [astro-ph.CO] (2009)
99. Hoyle F. *Astrophys. J. Suppl.* 1:121 (1954)
100. Feng JL. *Annu. Rev. Astron. Astrophys.* 48:495 (2010)
101. Hooper D, Baltz EA. *Annu. Rev. Nucl. Part. Sci.* 58:293 (2008)
102. Gaitskell RJ. *Annu. Rev. Nucl. Part. Sci.* 54:315 (2004)
103. Ellis J, Kim JE, Nanopoulos DV. *Phys. Lett.* B145:181 (1984)
104. Lindley D. *Astrophys. J.* 294:1 (1985)

105. Ellis J, Nanopoulos DV, Sarkar S. *Nucl. Phys. B* 259:175 (1985)
106. Juszkiewicz R, Silk J, Stebbins A. *Phys. Lett.* B158:463 (1985)
107. Kawasaki M, Sato K. *Phys. Lett.* B189:23 (1987)
108. Reno MH, Seckel D. *Phys. Rev. D* 37:3441 (1988)
109. Scherrer RJ, Turner MS. *Astrophys. J.* 331:19 (1988)
110. Dimopoulos S, Esmailzadeh R, Hall LJ, Starkman GD. *Nucl. Phys. B* 311:699 (1989)
111. Ellis J, et al. *Nucl. Phys. B* 373:399 (1992)
112. Moroi T, Murayama H, Yamaguchi M. *Phys. Lett.* B303:289 (1993)
113. Jedamzik K. *Phys. Rev. D* 74:103509 (2006)
114. Cyburt RH, Ellis J, Fields BD, Olive KA. *Phys. Rev. D* 67:103521 (2003)
115. Kawasaki M, Kohri K, Moroi T. *Phys. Rev. D* 71:083502 (2005)
116. Pospelov M. *Phys. Rev. Lett.* 98:231301 (2007)
117. Jedamzik K. *Phys. Rev. D* 70:083510 (2004)
118. Jedamzik K. *Phys. Rev. D* 70:063524 (2004)
119. Jedamzik K, Choi K, Roszkowski L, Ruiz de Austri R. *J. Cosmol. Astropart. Phys.* 7:7 (2006)
120. Kusakabe M, et al. *Phys. Rev. D* 76:121302 (2007)
121. Pospelov M, Pradler J, Steffen FD. *J. Cosmol. Astropart. Phys.* 11:20 (2008)
122. Jedamzik K. *Phys. Rev. D* 77:063524 (2008)
123. Bailly S, Jedamzik K, Moultaka G. *Phys. Rev. D* 80:063509 (2009)
124. Peskin ME. *Supersymmetry in Elementary Particle Physics.* Cambridge, UK: Cambridge Univ. Press. 609 pp. (2008)
125. Olive KA. In *The Primordial Universe*, ed. P Binétruy, R Schaeffer, J Silk, F David, p. 221. Berlin: Springer (2010)
126. Martin SP. In *Perspectives on Supersymmetry*, ed. GL Kane, p. 1. New York: World Sci. (1998)
127. Ellis J, et al. *Nucl. Phys. B* 238:453 (1984)
128. Ellis J, Olive KA, Santoso Y, Spanos VC. *Phys. Lett.* B565:176 (2003)
129. Kamimura M, Kino Y, Hiyama E. *Prog. Theor. Phys.* 121:1059 (2009)
130. Kusakabe M, Kajino T, Yoshida T, Mathews GJ. *Phys. Rev. D* 81:083521 (2010)
131. Bird C, Koopmans K, Pospelov M. *Phys. Rev. D* 78:083010 (2008)
132. Kusakabe M, et al. *Astrophys. J.* 680:846 (2008)
133. Cyburt RH, et al. *J. Cosmol. Astropart. Phys.* 11:14 (2006)
134. Kawasaki M, Kohri K, Moroi T, Yotsuyanagi A. *Phys. Rev. D* 78:065011 (2008)
135. Kohri K, Takahashi T. *Phys. Lett.* B682:337 (2010)
136. Uzan J. *Rev. Mod. Phys.* 75:403 (2003)
137. Flambaum VV, Shuryak EV. *Phys. Rev. D* 67:083507 (2003)
138. Flambaum VV, Wiringa RB. *Phys. Rev. C* 76:054002 (2007)
139. Coc A, et al. *Phys. Rev. D* 76:023511 (2007)
140. Berengut JC, Flambaum VV, Dmitriev VF. *Phys. Lett.* B683:114 (2010)
141. Coc A, Olive KA, Uzan J, Vangioni E. *Phys. Rev. D* 79:103512 (2009)
142. Flambaum VV, Shuryak EV. *Phys. Rev. D* 65:103503 (2002)
143. Dmitriev VF, Flambaum VV, Webb JK. *Phys. Rev. D* 69:063506 (2004)
144. Moffat JW. *J. Cosmol. Astropart. Phys.* 5:1 (2006)
145. Regis M, Clarkson C. arXiv:1003.1043 [astro-ph.CO] (2010)
146. Holder GP, Nollett KM, van Engelen A. *Astrophys. J.* 716:907 (2010)
147. Piau L, et al. *Astrophys. J.* 653:300 (2006)
148. Fields BD, et al. *Astrophys. J.* 563:653 (2001)
149. Vangioni E, Silk J, Olive KA, Fields BD. *Mon. Not. R. Astron. Soc.* In press (2011)

Annual Review of Nuclear and Particle Science

Volume 61, 2011

Contents

Neutral Pion Decay
R. Miskimen 1

Symmetry Tests in Nuclear Beta Decay
Nathal Severijns and Oscar Naviliat-Cuncic 23

The Primordial Lithium Problem
Brian D. Fields 47

Neutrino Mass in Cosmology: Status and Prospects
Yvonne Y.Y. Wong 69

Computing for the Large Hadron Collider
Ian Bird 99

Semileptonic *B* Meson Decays
Vera G. Lüth 119

Particle Physics Outreach to Secondary Education
Marjorie G. Bardeen, K. Erik Johansson, and M. Jean Young 149

Observation of Single Top Quark Production
Ann Heinson and Thomas R. Junk 171

Advances in Tracking Detectors
Frank Hartmann and Jochen Kaminski 197

Diboson Production at Colliders
Mark S. Neubauer 223

Supernova Cosmology: Legacy and Future
Ariel Goobar and Bruno Leibundgut 251

Multivariate Analysis Methods in Particle Physics
Pushpalatha C. Bhat 281

Associated Production of *W/Z* Gauge Bosons and Jets in Hadronic Collisions
John Campbell and Michelangelo Mangano 311

Rare Kaon and Pion Decays: Incisive Probes for New Physics Beyond the Standard Model
Douglas Bryman, William J. Marciano, Robert Tschirhart, and Taku Yamanaka 331

Neutrino-Nucleus Interactions
H. Gallagher, G. Garvey, and G.P. Zeller 355

Higgs Boson Searches at the Tevatron
Matthew Herndon 379

Spin-Dependent Electron Scattering from Polarized Protons and Deuterons with the BLAST Experiment at MIT-Bates
Douglas K. Hasell, Richard G. Milner, Robert P. Redwine, Ricardo Alarcon, Haiyan Gao, Michael Kohl, and John R. Calarco 409

The Large Hadron Collider
Lyndon Evans 435

Extensive Air Showers and Hadronic Interactions at High Energy
Ralph Engel, Dieter Heck, and Tanguy Pierog 467

Physics Opportunities at the Next Generation of Precision Flavor Physics Experiments
Marco Ciuchini and Achille Stocchi 491

Indexes

Cumulative Index of Contributing Authors, Volumes 52–61 519

Cumulative Index of Chapter Titles, Volumes 52–61 523

Errata

An online log of corrections to *Annual Review of Nuclear and Particle Science* articles may be found at http://nucl.annualreviews.org/errata.shtml